



# CHORUS

This is the accepted manuscript made available via CHORUS. The article has been published as:

## Auxiliary-field quantum Monte Carlo method for strongly paired fermions

J. Carlson, Stefano Gandolfi, Kevin E. Schmidt, and Shiwei Zhang

Phys. Rev. A **84**, 061602 — Published 7 December 2011

DOI: [10.1103/PhysRevA.84.061602](https://doi.org/10.1103/PhysRevA.84.061602)

# Auxiliary-Field Quantum Monte Carlo for Strongly Paired Fermions

J. Carlson,<sup>1</sup> Stefano Gandolfi,<sup>1</sup> Kevin E. Schmidt,<sup>2</sup> and Shiwei Zhang<sup>3</sup>

<sup>1</sup>*Theoretical Division, Los Alamos National Laboratory, Los Alamos, NM 87545, USA*

<sup>2</sup>*Department of Physics, Arizona State University, Tempe, AZ 85287, USA*

<sup>3</sup>*Department of Physics, College of William and Mary, Williamsburg, VA 23187, USA*

We solve the zero-temperature Unitary Fermi Gas problem by incorporating a BCS importance function into the Auxiliary-field quantum Monte Carlo method. We demonstrate that this method does not suffer from a sign problem, and that it increases the efficiency of standard techniques by many orders of magnitude for strongly-paired fermions. We calculate the ground-state energies exactly for unpolarized systems with up to 66 particles on lattices of up to  $27^3$  sites, obtaining an accurate result for the universal parameter  $\xi$ . We also obtain results for interactions with different effective ranges, and find that the energy is consistent with a universal linear dependence on the product of the Fermi momentum and the effective range. This new method will have many applications in superfluid cold atom systems and in both electronic and nuclear structures where pairing is important.

The study of strongly interacting Fermi systems is one of the central themes and major challenges in physics. Superfluidity in unpolarized cold atomic Fermi gases, which has been demonstrated both experimentally and theoretically, provides a prototypical example. The experimental ability to use a Feshbach resonance to adjust the strength of the potential between the atoms allows an exploration of the physics over many length scales. A particularly interesting regime is at unitarity where the scattering length diverges and the effective range of the potential is very small compared to the interparticle spacing. Since the particle density provides the only length scale, the ground-state energy  $E_0$  is proportional to the free Fermi gas energy  $E_{FG}$ ,

$$E_0 = \xi E_{FG}. \quad (1)$$

The ability to quantitatively understand the properties of this system represents a great triumph of many-body physics. Many experiments and calculations have been performed for the unitary Fermi gas. Initial qualitative agreement was found between theory[1, 2] and experiment[3–5]. More precise recent experiments have yielded  $\xi = 0.39(2)$ [6] and  $0.41(1)$ [7], with smaller values obtained very recently by Zwierlein, et al.[8]. Fixed-node Diffusion Monte Carlo (DMC) calculations[1, 2, 9–12] have always included a Bardeen-Cooper-Schrieffer[13] (BCS) trial wave function to guide the Monte Carlo walk and provide the fixed node constraint[14] needed to overcome the fermion sign problem. As is well known, these calculations provide an upper bound, with the current best value  $\xi = 0.383(1)$ [11, 12].

In this paper we show that *exact* calculations can be performed to accurately determine the ground-state properties of the unpolarized Fermi gas. Furthermore, we perform calculations with small but finite effective range, and find results consistent with a universal linear dependence of the energy upon the Fermi momentum times the effective range:  $E/E_{FG} = \xi + Sk_F r_e + \dots$

A new method is introduced to allow the use of a BCS

trial wave function in the auxiliary-field quantum Monte Carlo (AFQMC) approaches of Zhang and coworkers[15, 16]. Using the new approach, we perform calculations with several forms of the kinetic energy term that all give the correct continuum limit but with different finite effective ranges to study the convergence with particle number and lattice sizes, and to obtain the dependence of  $\xi$  on the effective range. An exact result is obtained for the value of  $\xi$ , as well as results for the slope  $S$ .

Quantum Monte Carlo simulations play a key role in addressing the challenge of strongly interacting Fermi systems. The AFQMC method has been applied to a variety of systems in several fields. With equal numbers and masses of up- and down-spin fermions and an attractive interaction, there is no fermion sign problem. The formalism developed here allows the use of a BCS importance function, which drastically improves the efficiency in this situation. In general applications, a sign or phase problem is present, which is controlled by a constraint, also using the importance function [15, 16]. Hartree-Fock or free Fermi gas (FG) type of importance functions have been used. This approach has been shown to be very accurate in many condensed matter models and optical lattices [17], quantum chemistry [18], and solid state materials [19]. The present method will allow the use of BCS importance functions (or antisymmetrized geminal power (AGP) in chemistry) to significantly improve our ability to deal with the sign problem in systems where pairing is important, and enhance the capabilities for quantum simulations in strongly correlated systems in general.

The AFQMC method, in both-zero[20] and finite-temperature formulations[21], has also been applied to the unitary Fermi gas. Precise results require simultaneously large lattices, so the system is dilute, and a large number of particles for an accurate approach to the continuum and thermodynamic limits. Many such calculations have been performed[20, 22–25], but the variance of the method limited the results to relatively small number of particles and lattice sizes so that, as we demonstrate

below, the results are unlikely to have converged to the thermodynamic limit.

The range of the van der Waals interaction in cold atoms is small (e.g. about 3 nm in  ${}^6\text{Li}$ [26]) compared to interparticle spacing so that the short range structure of the interaction is unimportant; the results are completely determined by the form of the kinetic energy and the scattering length. For an  $N_k^3$  lattice, the equivalent Hamiltonian is

$$H = \frac{1}{N_k^3} \sum_{\mathbf{k}, \mathbf{j}, \mathbf{m}, \mathbf{s}} \psi_{\mathbf{j}\mathbf{s}}^\dagger \psi_{\mathbf{m}\mathbf{s}} \epsilon_{\mathbf{k}} e^{i\mathbf{k}\cdot(\mathbf{r}_{\mathbf{j}} - \mathbf{r}_{\mathbf{m}})} + U \sum_i n_{i\uparrow} n_{i\downarrow}. \quad (2)$$

Here  $\psi_{\mathbf{j}\mathbf{s}}$  is the destruction operator for a fermion of spin  $s$  on lattice site at position  $\mathbf{r}_{\mathbf{j}}$ . For odd lattice sizes  $N_k = 2N_c + 1$ , the  $\mathbf{k}$  are given by  $\frac{2\pi}{L}(n_x\hat{\mathbf{x}} + n_y\hat{\mathbf{y}} + n_z\hat{\mathbf{z}})$  with  $-N_c \leq n_x, n_y, n_z \leq N_c$ . The  $k$  space destruction operators are  $c_{\mathbf{k}\mathbf{s}} = N_k^{-3/2} \sum_{\mathbf{j}} e^{-i\mathbf{k}\cdot\mathbf{r}_{\mathbf{j}}} \psi_{\mathbf{j}\mathbf{s}}$ , and the density operators are  $n_{i\mathbf{s}} = \psi_{i\mathbf{s}}^\dagger \psi_{i\mathbf{s}}$ .

To reach the continuum limit, we need to take the limit of zero particle density,  $\rho \equiv N/N_k^3 \rightarrow 0$ , in the context of the Hubbard model (i.e., replace  $L$  by  $N_k$ ). Equivalently, because of scale invariance, we can think of the system as a discretized representation of a supercell with fixed size  $L$ , and take the  $k$ -space cutoff to infinity. In either case, we then take the number of particles,  $N$ , to infinity. In this limit only the behavior of  $\epsilon_{\mathbf{k}}$  for  $k \ll \frac{2\pi}{\alpha}$  is important, where  $\alpha \equiv L/N_k$  is the lattice spacing. Thus a variety of kinetic energy forms can be used as long as they are quadratic for  $k$  much smaller than the cutoff. In this work we present results for

$$\begin{aligned} \epsilon_{\mathbf{k}}^{(2)} &= \frac{\hbar^2 k^2}{2m}, & \epsilon_{\mathbf{k}}^{(4)} &= \frac{\hbar^2 k^2}{2m} [1 - \beta^2 k^2 \alpha^2] \\ \epsilon_{\mathbf{k}}^{(h)} &= \frac{\hbar^2}{m\alpha^2} [3 - \cos(k_x\alpha) - \cos(k_y\alpha) - \cos(k_z\alpha)]. \end{aligned} \quad (3)$$

The superscript 2 and 4 indicate the highest power of  $k$ , while  $\epsilon_{\mathbf{k}}^{(h)}$  is the Hubbard model hopping kinetic energy offset by a constant so that it is zero at  $\mathbf{k} = 0$ .

For two particles, the Hamiltonian is separable, and the solution of the Lippmann-Schwinger equation for low-energy s-wave scattering gives the phase-shift equation,

$$k \cot \delta_0 = -\frac{4\pi\hbar^2}{mU\alpha^3} \left[ 1 + \frac{U\alpha^3}{16\pi^3} \mathcal{P} \int_{-\pi/\alpha}^{\pi/\alpha} dk'_x \int_{-\pi/\alpha}^{\pi/\alpha} dk'_y \int_{-\pi/\alpha}^{\pi/\alpha} dk'_z \frac{1}{\epsilon_{\mathbf{k}'} - \epsilon_{\mathbf{k}}} \right] \quad (4)$$

where  $\mathcal{P}$  indicates the principal parts integration, and the  $k$  space sums are cut off by the lattice spacing  $\alpha$ . The effective range expansion is

$$k \cot \delta_0 = -a^{-1} + \frac{1}{2}k^2 r_e + \dots \quad (5)$$

where  $a$  is the scattering length and  $r_e$  the effective range. Since we are interested in the unitary limit, we adjust

$U$  to have  $a^{-1} = 0$ . Both  $\epsilon_{\mathbf{k}}^{(2)}$  and  $\epsilon_{\mathbf{k}}^{(h)}$  have nonzero effective ranges. The extra parameter  $\beta$  in  $\epsilon_{\mathbf{k}}^{(4)}$  can be adjusted to make the effective range zero. The values for the parameters are given in table I.

Energy	$U \frac{2m\alpha^2}{\hbar^2}$	$\beta$	$r_e \alpha^{-1}$
$\epsilon_{\mathbf{k}}^{(h)}$	-7.91355	-	-0.30572
$\epsilon_{\mathbf{k}}^{(2)}$	-10.28871	-	0.33687
$\epsilon_{\mathbf{k}}^{(4)}$	-8.66605	0.16137	0.00000

TABLE I. The parameters that give infinite scattering length for two particles in an infinite lattice for the various kinetic energies. The  $\beta$  value for the  $\epsilon_{\mathbf{k}}^{(4)}$  kinetic energy has been adjusted to give zero effective range,  $r_e$ .

The AFQMC algorithm uses branching random walks to project the ground state from an initial trial state with the imaginary-time operator  $\exp[-H\tau]$ . Because the interaction is attractive, there is no fermion sign problem for equal numbers of up and down fermions studied here, and no path constraint is required. A walker is a set of  $N$  single-particle orbitals. Initially, the orbitals for the up spin particles are taken to be identical to those for the down spin particles. The two-body interaction term is broken up using a Hubbard-Stratonovich (HS) transformation which has only positive weights, and treats the up and down spin particles identically. Therefore, the up spin orbitals remain identical to the down spin orbitals during the propagation. We will show below that the usual form for a singlet paired BCS trial function also gives no fermion sign problem.

The walker states are given by specifying the orbital coefficients. These can be specified on the real space lattice  $\phi_{n,\mathbf{j}}$  or as momentum space coefficients  $\tilde{\phi}_{n,\mathbf{k}}$  related to each other by a discrete Fourier transform. If we begin with real orbitals on the real space lattice, the orbitals remain real when propagated. The momentum space orbitals therefore satisfy  $\tilde{\phi}_{n,-\mathbf{k}} = \tilde{\phi}_{n,\mathbf{k}}^*$ . The orbitals are orthonormalized periodically. This is needed to limit roundoff error, but the mathematical expressions are correct without it. The orthonormal orbitals therefore satisfy  $\sum_{\mathbf{k}} \tilde{\phi}_{n,\mathbf{k}}^* \tilde{\phi}_{m,\mathbf{k}} = \delta_{nm}$ , and the corresponding operators,  $w_{n\mathbf{s}} = \sum_{\mathbf{k}} \tilde{\phi}_{n,\mathbf{k}} c_{\mathbf{k}\mathbf{s}}$ , satisfy  $\{w_{n\mathbf{s}}, w_{m\mathbf{s}'}^\dagger\} = \delta_{nm} \delta_{\mathbf{s}\mathbf{s}'}$ . The walker state is

$$|W\rangle = \prod_{n=1}^{N/2} w_{n\uparrow}^\dagger w_{n\downarrow}^\dagger |0\rangle. \quad (6)$$

Because  $N \ll N_k^3$  and because the imaginary-time history of the walk need not be retained, this formalism is much more efficient than the usual lattice formulations for the ground state of dilute gases.

Using a discrete HS transformation[27], the potential

energy propagator is

$$e^{-U \sum_i n_{i\uparrow} n_{i\downarrow} \Delta t} = \frac{1}{2^{N_k^3}} \sum_{\{\sigma\}=\pm 1} G_V(\{\sigma\}, \Delta t)$$

$$G_V(\{\sigma\}, \Delta t) = \exp \left[ \sum_{i,s} (2u\sigma_i - \frac{1}{2}U\Delta t) n_{is} - u\sigma_i \right] \quad (7)$$

where  $\tanh^2 u = -\tanh(\frac{U\Delta t}{4})$ . The kinetic energy propagator is

$$G_T(\Delta t) = \exp \left[ - \sum_{\mathbf{k}} \epsilon_{\mathbf{k}} \left( c_{\mathbf{k}\uparrow}^\dagger c_{\mathbf{k}\uparrow} + c_{\mathbf{k}\downarrow}^\dagger c_{\mathbf{k}\downarrow} \right) \Delta t \right]. \quad (8)$$

Given a choice of one of the  $N_k^3$  set of fields, the application of the Trotter breakup of one term of the propagator on a walker  $|W\rangle$  gives another walker  $|W'\rangle$  times a weight  $w'(\{\sigma\}, W)$  that depends on the set of HS variables  $\{\sigma\}$  and  $|W\rangle$ ,

$$G(\{\sigma\}, \Delta t)|W\rangle \equiv G_T(\frac{\Delta t}{2})G_V(\{\sigma\}, \Delta t)G_T(\frac{\Delta t}{2})|W\rangle \rightarrow w'(\{\sigma\}, W)|W'\rangle. \quad (9)$$

The propagation above consists of (1) Multiply each  $\tilde{\phi}_{n,\mathbf{k}}$  by  $\exp(-\frac{1}{2}\epsilon_{\mathbf{k}}\Delta t)$ . (2) Fast Fourier transform to obtain  $\phi_{n,i}$  in real space. (3) Multiply each  $\phi_{n,i}$  by  $\exp(2u\sigma_i - \frac{1}{2}U\Delta t)$ . (4) Fast Fourier transform to obtain  $\tilde{\phi}_{n,\mathbf{k}}$  in momentum space. (5) Multiply each  $\tilde{\phi}_{n,\mathbf{k}}$  by  $\exp(-\frac{1}{2}\epsilon_{\mathbf{k}}\Delta t)$ . (6) Update the weight from non-operator terms.

Including importance sampling reduces the fluctuations, by changing the sampling so that it is non-uniform, without biasing the results. We want to sample walkers  $|W\rangle$  from  $\langle \Psi_T | W \rangle \langle W | \psi(t) \rangle$  where

$$|\psi(t + \Delta t)\rangle = e^{-(H-E_T)\Delta t} |\psi(t)\rangle \quad (10)$$

The contribution of a walker  $|W\rangle$  at the next time step is then

$$\sum_{\{\sigma\}=\pm 1} \left[ \frac{1}{2^{N_k^3}} \frac{\langle \Psi_T | G(\{\sigma\}, \Delta t) | W \rangle}{\langle \Psi_T | W \rangle} e^{-E_T \Delta t} \right] \times \frac{1}{w(\{\sigma\}, W)} G(\{\sigma\}, \Delta t) | W \rangle. \quad (11)$$

We want to sample the set of HS variables  $\{\sigma\}$ , from the unnormalized probability distribution given by the square brackets. The normalization which, to order  $\Delta t^2$  is the local energy expression  $e^{-\frac{1}{2}[E_L(W)+E_L(W')-E_T]\Delta t}$ , will give the weight of the sampled walkers. Once we have sampled the  $\{\sigma\}$  values, the new normalized walker is given by the second term of Eq. 11. We make sure that regions where the trial function is small are sampled adequately to eliminate trial-function bias.

The particle projected BCS state is

$$|BCS\rangle = \left[ \sum_{\mathbf{k}} f_{\mathbf{k}} c_{\mathbf{k}\uparrow}^\dagger c_{-\mathbf{k}\downarrow}^\dagger \right]^{N/2} |0\rangle, \quad (12)$$

where  $f_{\mathbf{k}} = v_{\mathbf{k}}/u_{\mathbf{k}}$  in the usual notation. The overlap of a walker with the BCS state is

$$\langle W | BCS \rangle = \langle 0 | \prod_{n=1}^{N/2} w_{n\downarrow} w_{n\uparrow} \left[ \sum_{\mathbf{k}} f_{\mathbf{k}} c_{\mathbf{k}\uparrow}^\dagger c_{-\mathbf{k}\downarrow}^\dagger \right]^{N/2} |0\rangle \quad (13)$$

The contraction needed is  $\overline{w_{n\downarrow} c_{\mathbf{k}s}^\dagger} = \tilde{\phi}_{n,\mathbf{k}} \delta_{ss'}$ . The two creation operators in the BCS pair must be contracted with some  $w_{m\uparrow}$  and some  $w_{n\downarrow}$ , giving a term

$$A_{nm} = w_{n\downarrow} w_{m\uparrow} \sum_{\mathbf{k}} f_{\mathbf{k}} c_{\mathbf{k}\uparrow}^\dagger c_{-\mathbf{k}\downarrow}^\dagger$$

$$= \sum_{\mathbf{k}} \tilde{\phi}_{n,-\mathbf{k}} f_{\mathbf{k}} \tilde{\phi}_{m,\mathbf{k}} = \sum_{\mathbf{k}} \tilde{\phi}_{n,\mathbf{k}}^* f_{\mathbf{k}} \tilde{\phi}_{m,\mathbf{k}}. \quad (14)$$

Taking all the different possible full contractions,

$$\langle W | BCS \rangle = \det A, \quad (15)$$

where the elements of the  $\frac{N}{2} \times \frac{N}{2}$  matrix  $A$  are the  $A_{nm}$  of Eq. 14.

The overlap, Eq. 15, is positive when, as in the standard singlet paired BCS solutions,  $f_{\mathbf{k}} \geq 0$ . We write  $\det A = \det [BB^\dagger]$  where  $B^\dagger$  is the hermitian conjugate matrix of  $B$  and the matrix elements of the  $\frac{N}{2} \times N_k^3$  matrix  $B$  are  $B_{n\mathbf{k}} = \tilde{\phi}_{n,\mathbf{k}} \sqrt{f_{\mathbf{k}}}$ . Applying the Cauchy-Binet theorem, each of the determinants of the submatrices of  $B$  is multiplied by the determinant of the corresponding hermitian conjugate submatrix. The determinant of  $A$  is a sum of positive terms, so that our BCS trial function gives no sign problem.

Two estimates of the energy are used, the growth energy just measures the growth of the weights in the random walk. The local energy can be calculated using contractions similar to those above. Other observables can be calculated similarly. A complete derivation for a general BCS state will be published elsewhere. Here we give the result

$$E_L(W) = \frac{\langle W | H | BCS \rangle}{\langle W | BCS \rangle} = 2\text{tr} [A^{-1}C]$$

$$+ U \sum_{\mathbf{q}} \{ \text{tr} [A^{-1}E(\mathbf{q})] \text{tr} [A^{-1}E^\dagger(\mathbf{q})]$$

$$- \text{tr} [A^{-1}E(\mathbf{q})A^{-1}E^\dagger(\mathbf{q})] + \text{tr} [A^{-1}D(\mathbf{q})] \}, \quad (16)$$

where  $D_{nm}(\mathbf{q}) = \sum_{\mathbf{k}} \tilde{\phi}_{n,\mathbf{k}+\mathbf{q}}^* f_{\mathbf{k}} \tilde{\phi}_{m,\mathbf{k}+\mathbf{q}}$ ,  $C_{nm} = \sum_{\mathbf{k}} \tilde{\phi}_{n,\mathbf{k}}^* \epsilon_{\mathbf{k}} f_{\mathbf{k}} \tilde{\phi}_{m,\mathbf{k}}$ , and  $E_{nm}(\mathbf{q}) = \sum_{\mathbf{k}} \tilde{\phi}_{n,\mathbf{k}+\mathbf{q}}^* f_{\mathbf{k}} \tilde{\phi}_{m,\mathbf{k}}$ . The matrix elements of  $D$  and  $E$  are convolutions which

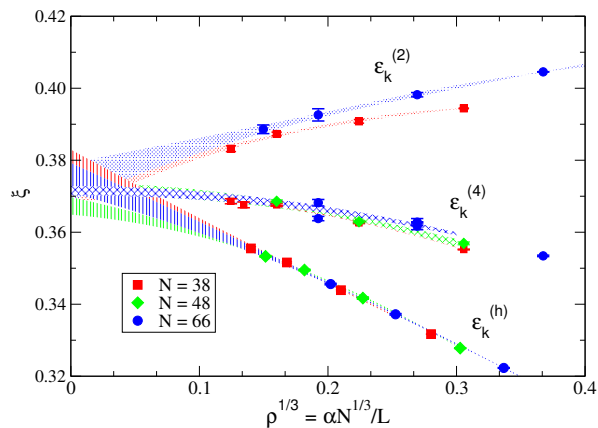


FIG. 1. (color online) The calculated ground state energy shown as the value of  $\xi$  versus the lattice size for various particle numbers and Hamiltonians.

are efficiently computed with fast Fourier transforms. The computational cost of using the BCS  $|\Psi_T\rangle$  is similar to using a single Slater determinant.

We have calculated the ground-state energy for different particle numbers and lattice sizes. The time-step errors have been extrapolated to zero within statistical errors, and walker population biases have been checked and were found to be negligible for the population sizes used. The imaginary time step is  $\approx 0.01 - 0.05 E_F^{-1}$ , the total propagation time is of order  $10 - 30 E_F^{-1}$  and 2,000-20,000 random walkers are used in the simulations.

For  $N = 4$ , we found that the use of BCS importance functions reduced the statistical error by a factor of 10, or  $100\times$  reduction in computer time, compared to the usual FG importance function. The improvement increased to  $1500\times$  for  $N = 38$  in a  $12^3$  lattice. For larger systems, the discrepancy is much larger still; indeed the statistical fluctuations from the latter are such that often meaningful results cannot be obtained with the run configurations described above.

In Fig. 1 we summarize our calculations of the energy as a function of  $\rho^{1/3}$  where  $\rho = N/N_k^3$ , and the particle number is  $N = 38, 48$  or  $66$ . We plot  $\xi$ , Eq. 1, where we have in all cases used the infinite system free-gas energy  $E_{FG} = \frac{3}{5} \frac{\hbar^2 k_F^2}{2m}$  with  $k_F^3 = 3\pi^2 \frac{N}{\alpha^3 N_k^3}$  as the reference.

DMC calculations have found converged results when using 66 particles[11, 12], and our results confirm this. The differences between 38 and 66 particles are rather small. Our calculations with 14 particles show a significant size dependence, and with 26 particles the effects are still noticeable. These are not shown on the figure. We have also computed the energy for 4 particle systems for a variety of lattice sizes and find agreement with Ref. [25]. The error bands in the figure provide least-squares estimates for the one sigma error based upon quadratic fits to the finite-size effects. The fits are of the form  $E/E_{FG} = \xi + A\rho^{1/3} + B\rho^{2/3}$ . For the interactions tuned

Hamiltonian	$N$	$\xi$	err	$A$	err
$\epsilon_k^{(2)}$	14	0.39	0.01	0.21	0.12
	38	0.370	0.005	0.14	0.04
	66	0.374	0.005	0.11	0.04
$\epsilon_k^{(4)}$	38	0.372	0.002		
	48	0.372	0.003		
	66	0.372	0.003		
$\epsilon_k^{(h)}$	4	0.280	0.004	-0.28	0.05
	38	0.380	0.005	-0.17	0.03
	48	0.367	0.005	-0.05	0.03
	66	0.375	0.005	-0.13	0.03

TABLE II. Energy extrapolations to infinite volume, zero range limit for various particle numbers  $N$  and different Hamiltonians. The term linear in the effective range,  $A$ , is also shown where it is not tuned to zero.

to  $r_e = 0$ , a fit with  $A$  fixed to zero is used. Including a linear coefficient in the fit yields a value statistically consistent with zero.

The extrapolation in lattice size for the  $k^2$  and Hubbard dispersions show opposite slope as expected from the opposite signs of their effective ranges. The extrapolation to  $\rho \rightarrow 0$  is consistent with  $\xi = 0.372(0.005)$  in all cases. Our final error contains statistical component and the errors associated with finite population sizes and finite time-step errors. This value is below previous experiments, but more compatible with recent experimental results of the Zwierlein group[8].

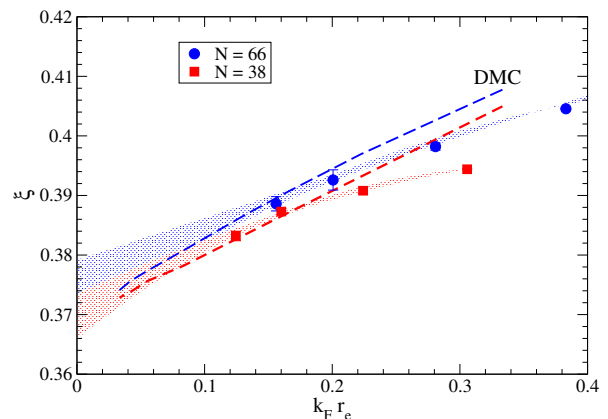


FIG. 2. (color online) The ground-state energy as a function of  $k_F r_e$ : comparison of DMC and AFQMC results. Dashed lines are DMC results, shifted down by 0.02 to enable comparison of the slopes.

We have also examined the behavior of the energy as a function of  $k_F r_e$  for finite effective ranges. The available length scales at low energy restrict  $\xi$  to be a function of  $k_F a$ ,  $k_F r_e$ ,  $k_F L$ , and  $k_F \alpha$ . At unitarity  $(k_F a)^{-1} = 0$ .  $(k_F L)^{-3}$  is proportional to  $N^{-1}$  so for large enough number of particles it can be neglected. The lattice has inversion symmetry so we expect a lowest order contribu-

tion proportional to  $(k_F \alpha)^2$ . Therefore the only linear in  $k_F$  correction to  $\xi$  is proportional to  $k_F r_e$ . It has been conjectured[28, 29] that the slope of  $\xi$  is universal in continuum Hamiltonians:  $\xi(r_e) = \xi + S k_F r_e$ . Of course a finite range purely attractive interaction is subject to collapse for a many-particle system, but a small repulsive many-body interaction or the lattice, where double occupancy of a single species is not allowed, is enough to stabilize the system. Our results are consistent with the universality conjecture. In particular our results for zero effective range approach the continuum limit with a slope consistent with zero.

Figure 2 compares the AFQMC results for the  $\epsilon_k^{(2)}$  interaction with the DMC results [11, 12] for various values of the effective range. The AFQMC produces somewhat lower energies than the DMC, consistent with the upper-bound nature of the DMC calculations. For the slope  $S$  of  $\xi$  with respect to finite  $r_e$ , the fit to the  $N = 66$  AFQMC results yields  $S = 0.11(.03)$ . Similar fits to the AFQMC data with the Hubbard dispersion  $\epsilon_k^{(h)}$  for  $N = 66$  yield a linear term of  $S = 0.12(.03)$ . Both are in agreement with the DMC results of  $S = 0.12(.01)$ . [30]

In summary, we have developed a new exact lattice technique to treat strongly-paired fermion systems. We find that the energy of the Fermi Gas at unitarity and zero effective range is  $\xi = 0.372(.005)$  using a variety of interactions tuned to unitarity. We also find results consistent with a universal dependence of the ground state energy upon the effective range:  $E/E_{FG} = \xi + S k_F r_e + \dots$  with  $S = 0.12(.03)$  for the different lattice and continuum Hamiltonians. The method we describe should be useful without modification for the entire BCS/BEC transition and for studying many other properties of cold Fermi gases. It can also be applied to a wide variety of problems in other strongly-correlated fermions, in areas ranging from cold atoms to condensed matter to quantum chemistry to nuclear physics.

We thank Alexandros Gezerlis, Joaquin Drut and David B. Kaplan for useful discussions. JC and SZ thank the Institute for Nuclear Theory (INT) at the University of Washington for its hospitality. This work is supported by the U.S. Department of Energy, Office of Nuclear Physics, under contracts DE-FC02-07ER41457 (UNEDF SciDAC), and DE-AC52-06NA25396 and by the National Science Foundation grants PHY-0757703, PHY-1067777. KES thanks the Los Alamos National Laboratory and the New Mexico Consortium for their hospitality. Computer time was also made available by Los Alamos Open Supercomputing, NERSC, and CPD at William & Mary. We thank Chia-Chen Chang for help with computing and coding issues. SZ is supported by ARO (56693-PH) and NSF (DMR-1006217).

- Chang, V. R. Pandharipande, J. Carlson, and K. E. Schmidt, Phys. Rev. A **70**, 043602 (2004).
- [2] G. Astrakharchik, J. Boronat, J. Casulleras, and S. Giorgini, Phys. Rev. Lett. **93**, 200404 (2004).
- [3] M. Bartenstein, A. Altmeyer, S. Riedl, S. Jochim, C. Chin, J. H. Denschlag, and R. Grimm, Phys. Rev. Lett. **92**, 203201 (2004).
- [4] J. Kinast, A. Turlapov, J. E. Thomas, Q. Chen, J. Stajic, and K. Levin, Science **307**, 1296 (2005).
- [5] G. B. Partridge, W. Li, R. I. Kamar, Y.-a. Liao, and R. G. Hulet, Science **311**, 503 (2006).
- [6] L. Luo and J. E. Thomas, J. Low Temp. Phys. **154**, 1 (2009).
- [7] N. Navon, S. Nascimbène, F. Chevy, and C. Salomon, Science **328**, 729 (2010).
- [8] M. W. Zwierlein(2011), talk presented at the Fermions from Cold Atoms to Neutron Stars Experimental Symposium, Institute for Nuclear Theory, Seattle, WA, May 16-20 2011.
- [9] J. Carlson and S. Reddy, Phys. Rev. Lett. **95**, 060401 (2005).
- [10] C. Lobo, I. Carusotto, S. Giorgini, A. Recati, and S. Stringari, Phys. Rev. Lett. **97**, 100405 (2006).
- [11] M. M. Forbes, S. Gandolfi, and A. Gezerlis, Phys. Rev. Lett. **106**, 235303 (2011).
- [12] S. Gandolfi, K. E. Schmidt, and J. Carlson, Phys. Rev. A **83**, 041601 (2011).
- [13] J. Bardeen, L. N. Cooper, and J. R. Schrieffer, Phys. Rev. **108**, 1175 (1957).
- [14] J. B. Anderson, J. Chem. Phys. **65**, 4121 (1976).
- [15] S. Zhang, J. Carlson, and J. E. Gubernatis, Phys. Rev. Lett. **74**, 3652 (1995); Phys. Rev. B **55**, 7464 (1997).
- [16] S. Zhang and H. Krakauer, Phys. Rev. Lett. **90**, 136401 (2003).
- [17] C.-C. Chang and S. Zhang, Phys. Rev. Lett. **104**, 116402 (2010).
- [18] W. A. Al-Saidi, S. Zhang, and H. Krakauer, J. Chem. Phys. **124**, 224101 (2006).
- [19] W. Purwanto, H. Krakauer, and S. Zhang, Phys. Rev. B **80**, 214116 (2009).
- [20] D. Lee, Phys. Rev. B **73**, 115112 (2006).
- [21] A. Bulgac, J. E. Drut, and P. Magierski, Phys. Rev. Lett. **96**, 090404 (2006).
- [22] D. Lee, Phys. Rev. B **75**, 134502 (2007).
- [23] D. Lee, Phys. Rev. C **78**, 024001 (2008).
- [24] D. Lee, Eur. Phys. J. A **35**, 171 (2008).
- [25] S. Bour, X. Li, D. Lee, U.-G. Meissner, and L. Mitas, Phys. Rev. A **83**, 063619 (2011).
- [26] W. Ketterle and M. W. Zwierlein, in *Ultracold Fermi Gases*, edited by M. Inguscio, W. Ketterle, and C. Salomon (IOSPress, Amsterdam, 2008) arXiv:0801.2500v1.
- [27] J. E. Hirsch, Phys. Rev. B **28**, 4059 (1983).
- [28] F. Werner and Y. Castin(2010), arXiv:1001.0774.
- [29] Y. Castin and F. Werner(2011), arXiv:1103.2851.
- [30] S. Gandolfi(2011), fig. 2 includes updated DMC results at small  $r_e$ .

---

[1] J. Carlson, S.-Y. Chang, V. R. Pandharipande, and K. E. Schmidt, Phys. Rev. Lett. **91**, 050401 (2003); S. Y.